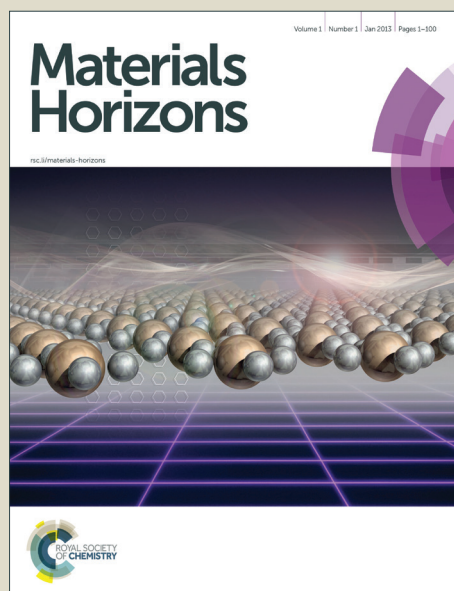


Materials Horizons

Accepted Manuscript



This is an *Accepted Manuscript*, which has been through the Royal Society of Chemistry peer review process and has been accepted for publication.

Accepted Manuscripts are published online shortly after acceptance, before technical editing, formatting and proof reading. Using this free service, authors can make their results available to the community, in citable form, before we publish the edited article. We will replace this *Accepted Manuscript* with the edited and formatted *Advance Article* as soon as it is available.

You can find more information about *Accepted Manuscripts* in the [Information for Authors](#).

Please note that technical editing may introduce minor changes to the text and/or graphics, which may alter content. The journal's standard [Terms & Conditions](#) and the [Ethical guidelines](#) still apply. In no event shall the Royal Society of Chemistry be held responsible for any errors or omissions in this *Accepted Manuscript* or any consequences arising from the use of any information it contains.

Spatial Atmospheric Atomic Layer Deposition: A new laboratory and industrial tool for low-cost photovoltaics

David Muñoz-Rojas^{1,2,3,*} & Judith MacManus-Driscoll³

1.- Instituto de Ciencia de Materiales de Barcelona, ICMAB-CSIC, Campus de la UAB, Bellaterra, 08193, SPAIN

2.- Laboratoire des Matériaux et du Génie Physique (LMGP), UMR 5628 CNRS – Grenoble INP Minatec, 3, Parvis Louis Néel MINATEC CS 50257, 38016 GRENOBLE Cedex 1, FRANCE.

3.- Department of Materials Science and Metallurgy, 27 Charles Babbage Road, University of Cambridge, Cambridge CB3 0FS, UK

* Corresponding author: davidmunozrojas@gmail.com

Abstract

Recently, a new approach to atomic layer deposition (ALD) has been developed that doesn't require vacuum and is much faster than conventional ALD. This is achieved by separating the precursors in space rather than in time. This approach is most commonly called Spatial ALD (SALD). In our lab we have been using/developing a novel atmospheric SALD system to fabricate active components for new generation solar cells, showing the potential of this novel technique for the fabrication of high quality materials that can be integrated into devices. In this minireview we will introduce the basics of SALD and illustrate its great potential by highlighting recent results in the field of photovoltaics.

Atomic Layer Deposition: unique pros, significant cons

Atomic Layer Deposition (ALD) is a powerful deposition technique offering unique assets: deposition of high quality films at low temperatures, very precise control over film thickness and highly conformal coatings, i.e. complete and uniform coating of high aspect ratio features.

These properties have rendered ALD the technique of choice in the microelectronics industry (e.g. deposition of gap dielectrics for magnetic heads, high-k oxide dielectrics and metal electrodes for Dynamic random-access memories, DRAM).¹⁻⁴ But the burst of nanoscience and nanotechnology in the last decades has also brought an associated boom of ALD popularity, since it allows the nanoengineering of surfaces with precise nanoscale control. As an example, the first report on the homogenous coating of nanoparticles by ALD dates from 2000,⁵ In the case of nanoparticles, a fluidized bed reactor is more convenient.⁶ This increase in the use of ALD is testified by the publication of 7 general reviews dedicated to ALD in the last decade.^{3,7-12} Apart from those, reviews have been written covering the application of ALD in specific areas such as nanotechnology,^{13,14} the environment¹⁵ and energy (lithium batteries,¹⁶ fuel cells¹⁷ and photovoltaics^{18,19}), and medical and biologic applications.²⁰ Despite this increasing success, ALD still faces two main drawbacks which compromise both its generalised use in the laboratory and its implementation in large scale, high throughput production lines. First, ALD is a very slow technique (up to 2 orders of magnitude slower than chemical vapour deposition (CVD)) and, second, it usually involves processing in vacuum, thus making it complicated and expensive to scale up.

Both the unique advantages and drawbacks of ALD are the consequence of how it works: ALD is a particular case of CVD in which the reaction is restricted to the sample surface, thus being self-limited. This is achieved by exposing the sample to the reactants at different time,²¹ i.e. in a sequence of pulses (figure 1a). In this way, the metal precursors (e.g. $\text{Al}(\text{CH}_3)_3$ in the case of fabrication of Al_2O_3) are supplied and react with the surface, ideally forming a monolayer. Excess precursor is then purged, usually by evacuation. The second precursor (e.g. H_2O) is then injected and reacts with the chemisorbed layer forming a monolayer of the desired material (i.e. Al_2O_3) plus by-products (CH_4) that have to be purged along with the excess precursor. The cycle is then repeated the necessary number of times to obtain a very precise film thickness. Thus, the unique advantages and drawbacks of conventional ALD are a consequence of

separating the different precursors in time (figure 1a, conventional ALD is thus also called *temporal* ALD).

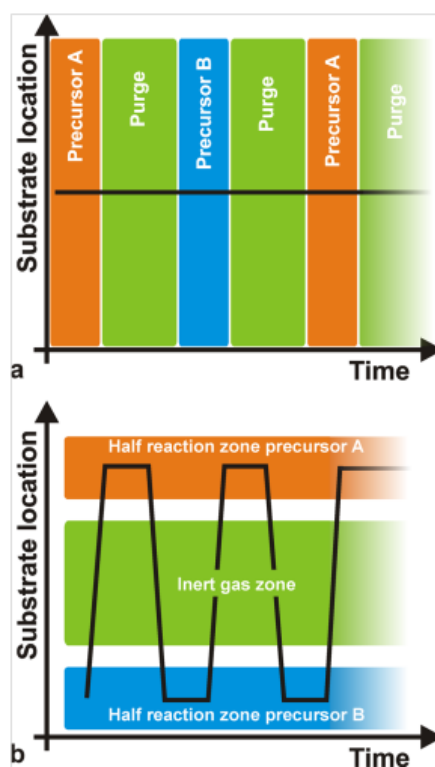


Figure 1a and b: Temporal vs. Spatial ALD. Copyright 2011, AIP Publishing LLC; Reprinted with permission from ref. ²²

The Key to atmospheric, high throughput ALD: from temporal to spatial

Although there have been several approaches to realizing ALD without the need of a high vacuum, *Spatial* ALD (SALD) has been the most popular in the last years due to its conceptual simplicity and the high deposition rates that can be achieved, and thus has also been called Atmospheric ALD (AALD).²³ Conversely, atmospheric temporal ALD approaches based on fluidized reactors show comparable deposition rates with conventional vacuum ALD since those still rely on injection-purge cycles.^{24–27} The key idea allowing high throughput atmospheric spatial ALD is not new and was indeed patented in 1977 and 1983 by Suntola et al.^{28,29} It simply consists in separating the precursors in space rather than in time (figure 1b), as

opposed to temporal ALD. Thus, in SALD the different precursors are supplied constantly in between inert gas regions. Films are then grown by alternatively exposing the substrate from one precursor region to the other going across the inert gas regions (figure 1b). In this way, the oscillation of the substrate (or of the gases injector) from one precursor zone to the second one, going across the inert gas regions, reproduces the classical temporal ALD scheme: the first metal precursor reacts with the surface forming a monolayer while any unreacted precursor is swept away and purged in the inert region; Then the second precursor reacts with the previous monolayer forming a layer of material; Finally the sample returns to the first precursor region again going across the inert region where any by-products and excess precursor are purged. This approach allows much faster deposition rates, which are mainly limited by the precursor reaction kinetics, so that a full reaction can take place while the sample is within the precursor zones. As recently reviewed by Poodt et al.²², from 2008 there has been a variety of SALD designs exploiting this idea, some of them already being commercialized. The versatility of Suntola's approach can be appreciated by the multiple designs and configurations presented so far.^{22,30}

One of the approaches used in several of the recent SALD designs is the use of a short distance between the precursor delivery zone and the substrate (typically below 100 μm , Figure 2a). In this configuration, referred to as "close proximity SALD", the different gas regions are located along alternative channels where the gases flow parallel to each other, as illustrated in Figure 2a. The close distance of the substrate, i.e. the small gap between injector and substrate, prevents the different precursors from mixing since the inert gas channel acts as an effective barrier. This approach has several advantages including: i) The possibility of having smaller designs since the precursor regions are very small; ii) Simpler designs which are compatible with roll-to-roll processing; iii) The possibility of using gas-bearings.²² Although several patents on close-proximity SALD were filed from 2008 to 2011,²² Levy et al. from Kodak were the first ones to present and publish their results on the deposition of ZnO thin film transistors, thus

showing the suitability of SALD for fabricating device components.³¹ Later Poedt et al. also demonstrated high quality Al_2O_3 films obtained by SALD. These films were used to passivate the surface of conventional silicon solar cells.³² The design used by Levy et al. consists of a deposition head in which the different gas flows are distributed along the parallel channels (see scheme in Figure 2b). This design is very simple and can be made very small, being indeed reminiscent of a printer head. Furthermore it is very easy to scale up, modify and customize. Finally, it is readily compatible with roll-to-roll processing. Such an approach is therefore very readily applicable both in laboratory and industrial settings. A similar approach has already been commercialized for the deposition of Al_2O_3 passivation layers on silicon and $\text{Cu}(\text{In,Ga})\text{Se}_2$ thin-film solar cells.^{22,33}

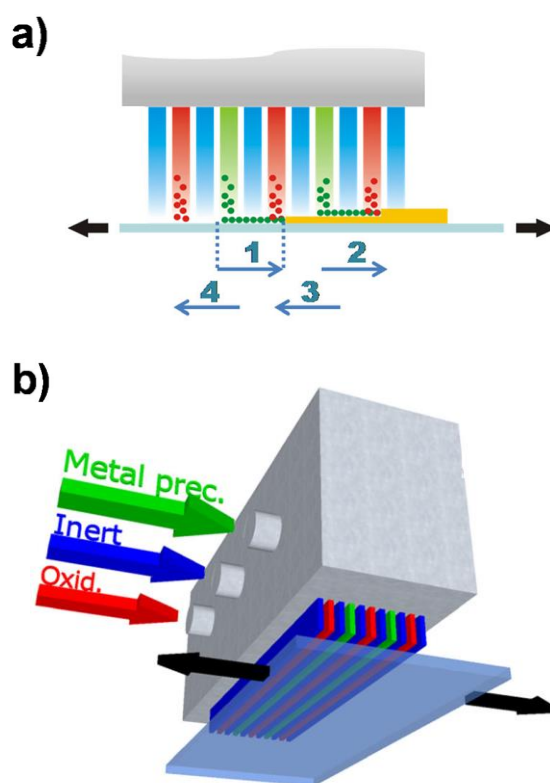


Figure 2. a) close-proximity SALD approach. The sample oscillates under the different flows reproducing the cycles in conventional ALD (numbered arrows); b) Scheme of the deposition head designed by Kodak. Copyright 2013 John Wiley & Sons, Ltd. Adapted with permission from ref.²³

The potential of SALD: Fabrication of active components for low-cost solar cells.

During the last years, in our group we have been using and developing a Kodak close-proximity SALD system, pioneering the deposition, study and implementation of high quality SALD films in low-cost/new generation photovoltaic devices.^{23,34-40} Our results include: i) The demonstration of the feasibility of using SALD for the ultra-fast deposition of high-quality films that can be integrated in devices; ii) The deposition of materials with superior properties compared to other low temperature and scalable methods; iii) The fundamental studies of new-generation solar cells by using doped oxide films; and iv) The nano-engineering of surfaces with SALD thin films to improve solar cells efficiencies. These results are succinctly reviewed next.

In the first example we used SALD to grow high quality TiO₂ blocking layers for organic (poly(3-hexylthiophene-2,5-diyl):[6,6]-phenyl-C61-butyric acid methyl ester (P3HT:PCBM)) solar cells.²³ Dense, uniform thin TiO₂ films were grown at temperatures as low as 100 °C in only 37 s (~20 nm/min growth rate). Incorporation of these films in P3HT-PCBM-based solar cells showed performances comparable with cells made using TiO₂ films deposited with much longer processing times and/or higher temperatures (SALD at 350 °C and spray pyrolysis at 450 °C). The high quality of the amorphous films obtained at 100 °C allowed the use of only 12 nm thick blocking layers, thus compensating for the lower conductivity of amorphous TiO₂ with respect to crystalline TiO₂, and resulting in two orders of magnitude faster deposition than other low-temperature scalable methods (figure 3a). We also studied thin ZnO (<200 nm) films grown by SALD in a matter of minutes as a hole-blocking layer in P3HT:PCBM based inverted solar cells. Despite the very rapid, open atmosphere growth method, the performances of the cells were comparable with the best cells of the same type reported in the literature. The performances were also maintained after 200 days of storage in air in the dark (figure 3b),³⁴ showing the high stability of the ZnO films made by SALD.

Secondly, we successfully deposited phase pure Cu_2O films of thickness 50 - 120 nm using our SALD system at temperatures between 125 and 225 °C (figure 3c, inset).³⁵ Growth rates were $\sim 1\text{nm}\cdot\text{min}^{-1}$, which is two orders of magnitude faster than conventional ALD. The films grown at 225 °C had carrier mobility values above $5\text{cm}^2\text{V}^{-1}\text{s}^{-1}$. Good carrier concentrations of around 10^{16}cm^{-3} were obtained for all deposition temperatures. The mobility values achieved were much higher than those obtained for electrodeposited films and approached the obtained for thermally oxidized films grown at 400 °C (figure 3c). Subsequently, we demonstrated SALD grown p+ Cu_2O films on top of electrodeposited $\text{ZnO}/\text{Cu}_2\text{O}$ solar cells (figure 3d) to build in the electric field, thereby permitting the use of a thinner ($\sim 1\text{mm}$ compared to $\sim 3\text{mm}$) electrodeposited Cu_2O layer. This thinner cell design gave reduced recombination losses and increased charge collection from both incident light and light reflected off the back electrode, resulting in a 29% increase in efficiency.³⁶

Another of the advantages of SALD is that doping can be achieved very easily by adding precursors to the different precursor lines. As an example, nitrogen doped ZnO ($\text{ZnO}:\text{N}$) can be deposited by using an ammonia solution instead of water.⁴¹ N doping decreases the carrier concentration of ZnO and this has allowed us to perform fundamental studies of PbX ($\text{X} = \text{S}, \text{Se}$) quantum dot (QD)/ZnO solar cells. For QDs where there is a significant density of intragap states, recombination at the ZnO/QD interface can be limited by reducing the ZnO carrier concentration through N doping since it prevents the back-transfer of electrons and/or enables the collection of trapped electrons via sub-bandgap states in the ZnO. As a result, both the cell open circuit voltage (V_{oc}) and efficiency increased with increasing N dopant level (figure 3e).³⁷ We have also used SALD to engineer the surface of ZnO by depositing a 20 nm coating of $\text{N}:\text{ZnO}$ on plain ZnO. The reduction in electron concentration in the surface results in enhanced exciton dissociation in $\text{ZnO}/\text{P3HT}$ cells due to a more efficient light-induced de-trapping of electrons for the $\text{ZnO}:\text{N}$ surface. This enhances exciton dissociation and electron transfer from

the P3HT to the oxide, resulting in 4 times higher short circuit density (figure 3f).³⁹ Finally, Mg doped ZnO has been successfully deposited using SALD, allowing a continuous tuning of the ZnO band gap from 3.3 eV to 5.5 eV by adjusting the Mg percentage in $Zn_{1-x}Mg_xO$. We then used $Zn_{1-x}Mg_xO$ in PbSe/ZnO solar cells, and we could increase the V_{oc} from 408 mV up to 608 mV at a $Zn_{1-x}Mg_xO$ bandgap of 3.55 eV, the highest V_{oc} reported to date for this type of cells (figures 3g-h).⁴⁰

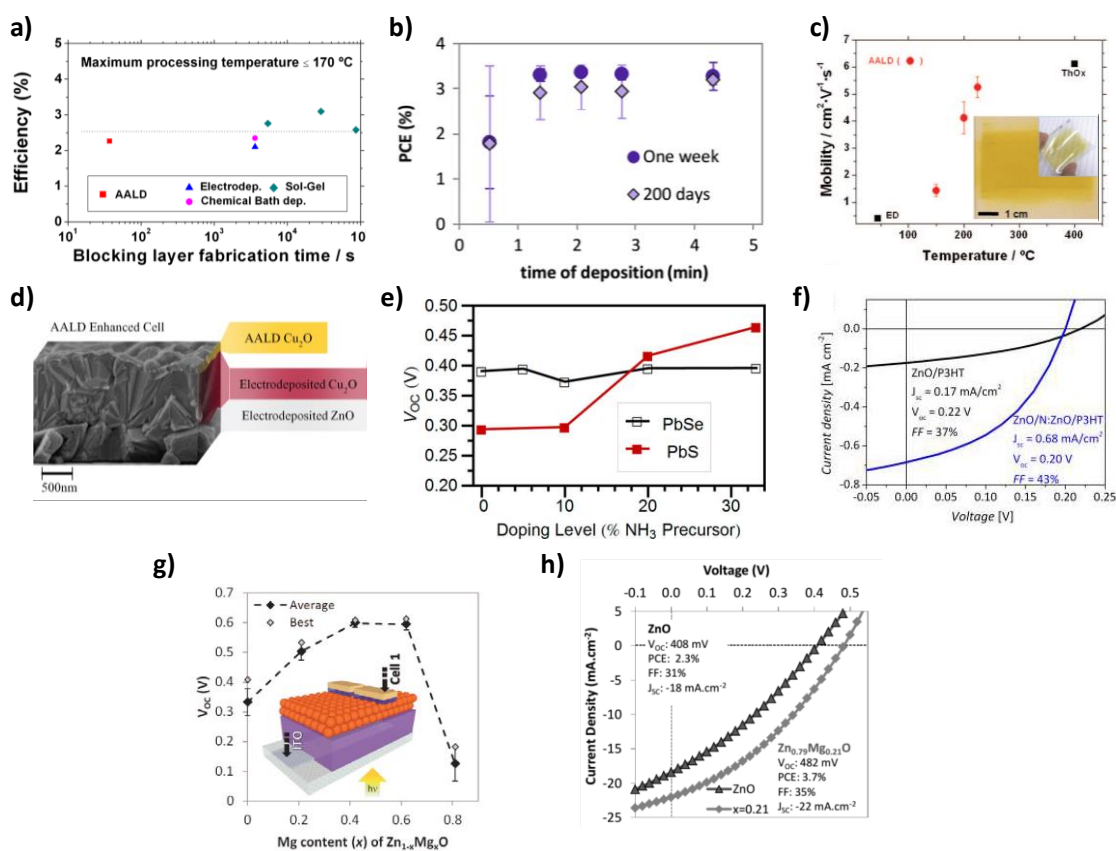


Figure 3: a) Best SALD cell efficiency compared with equivalent cells from the literature in terms of blocking layer fabrication time; Copyright 2013 John Wiley & Sons, Ltd. Reprinted with permission from ref.²³ b) Efficiency of devices with SALD ZnO hole-blocking layers measured one week after manufacture and 200 days after manufacture; Copyright 2013, Elsevier. Reprinted with permission from ref.³⁴ c) Mobility values as a function of temperature for SALD Cu_2O films compared to reported values for other non-vacuum methods (ED:

electrodeposition, ThOx: Thermal oxidation); inset: Optical photographs of Cu₂O films deposited at 150 °C on 6.3×6.3 cm² glass and flexible PEN substrates; Copyright 2012, American Institute of Physics. Licensed under Creative Commons Attribution 3.0 Unported. Reprinted from ref. ³⁵ d) Cross section SEM image of an SALD Cu₂O-enhanced electrodeposited ZnO/Cu₂O cell; Copyright Wiley-VCH Verlag GmbH & Co. KGaA. Reproduced with permission from ref. ³⁶ e) Open-circuit voltage of PbX(X = S,Se)/ZnO:N cells as a function of nitrogen-doping precursor fraction; Copyright 2013, American Chemical Society. Reprinted with permission from ref. ³⁷ f) Photovoltaic measurement of hybrid ZnO/P3HT devices employing approximately 60 nm ZnO films with and without a ZnO:N coating approximately 20 nm thick; Copyright Wiley-VCH Verlag GmbH & Co. KGaA. Reproduced with permission from ref. ³⁹ g) Open-circuit voltage (with device structure inset) for the Zn_{1-x}Mg_xO/PbSe cells over a doping series and h) Light *J-V* curves comparing the highest efficiency Zn_{1-x}Mg_xO-PbSe CQDSC with the most efficient ZnO-PbSe CQDSC ones. Copyright Wiley-VCH Verlag GmbH & Co. KGaA. Reproduced with permission from ref. ⁴⁰

Future challenges for SALD: towards a materials printer

SALD is a technique that has only just recently begun to be used for the deposition of high quality materials in functional devices. Indeed, the first theoretical⁴²⁻⁴⁴ and kinetic^{45,46} studies on SALD have been published in just the last months and reports evaluating the effect of deposition conditions on the properties of SALD ZnO and Al₂O₃ were also published recently.⁴⁷⁻
⁴⁹ To date, Al₂O₃, Cu₂O, TiO₂ and ZnO (including doping such as Al:ZnO, Mg:ZnO and ZnO:N) have already been demonstrated (table 1 presents a summary of these materials and the application to solar cells detailed above). Hence, while it is early days, it is clear that there is tremendous potential for SALD, as briefly discussed in this minireview. The emergence and importance of SALD has also been recognized by the inclusion of a dedicated symposium on high throughput ALD at the AVS60 meeting (Fall 2013).

Table 1: Summary of the different materials deposited by SALD to date and their application to photovoltaics†

Material	precursor	growth rate/ nm·s ⁻¹	growth rate/ nm·cycle ⁻¹	Deposition temperature / °C	reactor	sample size	Use in solar cells	Type of solar cell	Ref.
AZO	TMA, DEZ	0.20, 0.33	0.12, 0.2	200	L: TNO circular	3 cm	n.t.		50
Al ₂ O ₃	TMA	0.16	0.12	100	L: web coater	4 m x 100 mm	n.t.		30
	TMA	1.20	0.12	200	L: TNO circular	3 cm	barrier layer	Si, Cu(In,Ga)Se ₂	32,33
ZnO	DEZ	0.90	0.18	75-250	L: TNO circular	3 cm	n.t.		49
	DEZ	0.63	0.25	150	L: KCP	up to 15 cm ²	hole blocking layer	organic bulk heterojunction (P3HT/PCBM)	34
Mg:ZnO	DEZ, Mg(CpEt) ₂	0.28	0.2	150	L: KCP	up to 15 cm ²	n-type	Quantum dot (ZnO/PbSe)	40
ZnO:N	DEZ, NH ₃	0.36	0.16	150	L: KCP	up to 15 cm ²	n-type	Quantum dot (ZnO/PbX, X = S, Se)	37
								hybrid (ZnO/P3HT)	39
Cu ₂ O	Cupraselec t	0.02	0.006	150-225	L:KCP	up to 15 cm ²	p-type, hole doping	inorganic (ZnO/Cu ₂ O)	35,36
TiO ₂	TiCl ₄	0.32	0.15	100-350	L:KCP	up to 15 cm ²	hole blocking layer	organic bulk heterojunction (P3HT/PCBM)	23

† Abbreviations: AZO: aluminium doped zinc oxide, TMA: tetramethyl aluminium, DEZ: diethyl zinc, L: laboratory system, n.t.: not tested in solar cells, Mg(CpEt)₂: bis(ethylcyclopentadienyl)magnesium, TNO: Netherlands Organisation for Applied Scientific Research TNO, KCP: Kodak close proximity system; The growth rate per cycle refers to conventional ALD cycles, i.e. exposure to metal precursor followed by exposure to oxidant precursor. The relation between nm/cycle and nm/s depends both on each particular system and the deposition parameters used.

Despite this success, the ultimate challenge is to create a versatile materials printer based on the SALD approach where all the characteristics, materials and applications that are currently achievable with ALD can also be obtained with SALD, while maintaining the vacuum-free environment, use of simple equipment, and the orders of magnitude faster deposition rates.

One of the main limitations of SALD compared to ALD is that only relatively high volatility precursors can be used in order to have a sufficient amount of precursor molecules in the carrier gas. As the technique becomes more popular, we expect novel precursors to be designed specifically for SALD systems with higher volatility and reactivity. Of course, the price of novel SALD precursors will need to be reasonable in order not to compromise the low cost associated to SALD. But in this sense, SALD is intrinsically more efficient in terms of precursor utilisation, thus allowing the use of precursors with slightly higher prices than conventional ALD/CVD precursors. Other limitations that will have to be overcome include the ability to maintain the high deposition rates of SALD when high aspect ratio features have to be coated, since precursor diffusion plays a key role in these cases (particularly in the case of high aspect ratio cavities, such as supported alumina templates^{51,52}). The coating of freeform samples will require novel SALD designs, especially in the case of the close proximity approach. Additionally, while plasmas have already been implemented in some SALD systems,²² their use in atmospheric systems will have to be developed by implementing atmospheric plasmas. Finally, the deposition of complex materials such as multicomponent oxides remains to be explored using SALD.

One of the main advantages of SALD is that it is based on a very simple idea that allows for freedom of design modification, and that it is a very simple and cost-effective research tool, implementable in many different laboratory settings. Thus, customized systems for specific materials or substrates will surely be developed in the coming years. We expect that over the next years we will surely see a proliferation in the utilization of SALD, both in terms of the number of system designs and applications targeted – the areas of flextronics and barrier layer coatings being primary examples.

Acknowledgements

DMR acknowledges funding from the Marie Curie program (FP7/2007-2013, grant agreement number 219332), the Ramon y Cajal 2011 program from the Spanish MICINN and the European Social Fund, and the Comissionat per a Universitats i Recerca (CUR) del DIUE de la Generalitat de Catalunya, Spain. JLMD acknowledges the support of the European Research Council (ERC-2009-AdG 247276 NOVOX).

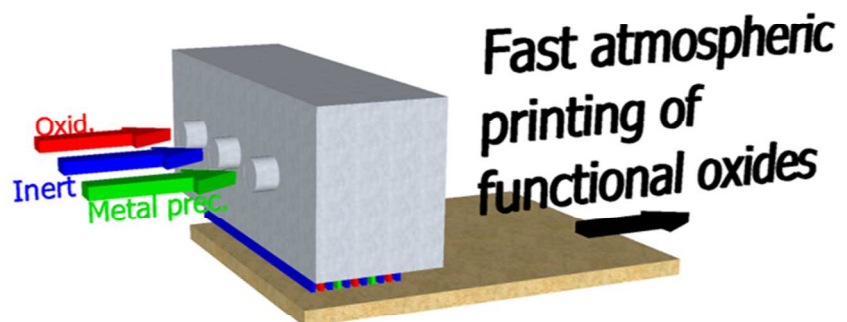
REFERENCES

1. R. G. Gordon, in *Atomic Layer Deposition for Semiconductors*, ed. C. S. Hwang, SPRINGER, 2013, p. 15.
2. T. Kääriäinen, D. Cameron, M.-L. Kääriäinen, and A. Sherman, in *Atomic Layer Deposition: Principles, Characteristics, and Nanotechnology Applications*, Wiley-Scrivener, 2nd edn., 2013, p. 215.
3. W. M. M. (Erwin) Kessels and M. Putkonen, *MRS Bull.*, 2011, **36**, 907–913.
4. G. N. Parsons, J. W. Elam, S. M. George, S. Haukka, H. Jeon, W. M. M. (Erwin) Kessels, M. Leskelä, P. Poodt, M. Ritala, and S. M. Rossnagel, *J. Vac. Sci. Technol. A Vacuum, Surfaces, Film.*, 2013, **31**, 050818.
5. J. Ferguson, A. Weimer, and S. George, *Thin Solid Films*, 2000, **371**, 95–104.
6. E. Rauwel, O. Nilsen, P. Rauwel, J. C. Walmsley, H. B. Frogner, E. Rytter, and H. Fjellvåg, *Chem. Vap. Depos.*, 2012, **18**, 315–325.
7. M. Leskelä and M. Ritala, *Thin Solid Films*, 2002, **409**, 138–146.
8. M. Leskelä and M. Ritala, *Angew. Chemie Int. Ed.*, 2003, **42**, 5548–5554.
9. R. L. Puurunen, *J. Appl. Phys.*, 2005, **97**, 121301.
10. G. Clavel, E. Rauwel, M.-G. Willinger, and N. Pinna, *J. Mater. Chem.*, 2009, **19**, 454.
11. S. M. George, *Chem. Rev.*, 2010, **110**, 111–131.
12. V. Miiikkulainen, M. Leskelä, M. Ritala, and R. L. Puurunen, *J. Appl. Phys.*, 2013, **113**, 021301.
13. M. Knez, K. Nielsch, and L. Niinistö, *Adv. Mater.*, 2007, **19**, 3425–3438.

14. D. M. King, X. Liang, and A. W. Weimer, *Powder Technol.*, 2012, **221**, 13–25.
15. C. Marichy, M. Bechelany, and N. Pinna, *Adv. Mater.*, 2012, **24**, 1017–32.
16. X. Meng, X.-Q. Yang, and X. Sun, *Adv. Mater.*, 2012, **24**, 3589–615.
17. M. Cassir, A. Ringuedé, and L. Niinistö, *J. Mater. Chem.*, 2010, **20**, 8987.
18. J. R. Bakke, K. L. Pickrahn, T. P. Brennan, and S. F. Bent, *Nanoscale*, 2011, **3**, 3482–508.
19. J. A. van Delft, D. Garcia-Alonso, and W. M. M. Kessels, *Semicond. Sci. Technol.*, 2012, **27**, 074002.
20. S. A. Skoog, J. W. Elam, and R. J. Narayan, *Int. Mater. Rev.*, 2013, **58**, 113–129.
21. M. Ritala and M. Leskelä, in *Handbook of Thin Film Materials*, ed. H. S. Nalwa, Academic Press, 2002, pp. 103–159.
22. P. Poodt, D. C. Cameron, E. Dickey, S. M. George, V. Kuznetsov, G. N. Parsons, F. Roozeboom, G. Sundaram, and A. Vermeer, *J. Vac. Sci. Technol. A Vacuum, Surfaces, Film.*, 2012, **30**, 010802.
23. D. Muñoz-Rojas, H. Sun, D. C. Iza, J. Weickert, L. Chen, H. Wang, L. Schmidt-Mende, and J. L. MacManus-Driscoll, *Prog. Photovoltaics Res. Appl.*, 2013, **21**, 393–400.
24. A. Hunter and A. H. Kitai, *J. Cryst. Growth*, 1988, **91**, 111–118.
25. R. Beetstra, U. Lafont, J. Nijenhuis, E. M. Kelder, and J. R. van Ommen, *Chem. Vap. Depos.*, 2009, **15**, 227–233.
26. J. S. Jur and G. N. Parsons, *ACS Appl. Mater. Interfaces*, 2011, **3**, 299–308.
27. A. Goulas and J. Ruud van Ommen, *J. Mater. Chem. A*, 2013, **1**, 4647.
28. T. S. Suntola, A. J. Pakkala, and S. G. Lindfors, 1983, US Patent 4,389,973.
29. T. S. Suntola and J. Antson, 1977, US Patent 4,058,430.
30. A. S. Yersak, Y. C. Lee, J. A. Spencer, and M. D. Groner, *J. Vac. Sci. Technol. A Vacuum, Surfaces, Film.*, 2014, **32**, 01A130.
31. D. H. Levy, D. Freeman, S. F. Nelson, P. J. Cowdery-Corvan, and L. M. Irving, *Appl. Phys. Lett.*, 2008, **92**, 192101.
32. P. Poodt, A. Lankhorst, F. Roozeboom, K. Spee, D. Maas, and A. Vermeer, *Adv. Mater.*, 2010, **22**, 3564–7.
33. A. Illiberi, F. Grob, C. Frijters, P. Poodt, R. Ramachandra, H. Winands, M. Simor, and P. J. Bolt, *Prog. Photovoltaics Res. Appl.*, 2013, **21**, 1559–1566.

34. R. L. Z. Hoye, D. Muñoz-Rojas, D. C. Iza, K. P. Musselman, and J. L. MacManus-Driscoll, *Sol. Energy Mater. Sol. Cells*, 2013, **116**, 197–202.
35. D. Muñoz-Rojas, M. Jordan, C. Yeoh, A. T. Marin, A. Kursumovic, L. Dunlop, D. C. Iza, A. Chen, H. Wang, and J. L. MacManus-driscoll, *AIP Adv.*, 2012, **2**, 042179.
36. A. T. Marin, D. Muñoz-Rojas, D. C. Iza, T. Gershon, K. P. Musselman, and J. L. MacManus-Driscoll, *Adv. Funct. Mater.*, 2013, **23**, 3413–3419.
37. B. Ehrler, K. P. Musselman, M. L. Böhm, F. S. F. Morgenstern, Y. Vaynzof, B. J. Walker, J. L. MacManus-Driscoll, and N. C. Greenham, *ACS Nano*, 2013, **7**, 4210–4220.
38. R. L. Z. Hoye, K. P. Musselman, and J. L. MacManus-Driscoll, *APL Mater.*, 2013, **1**, 060701.
39. K. P. Musselman, S. Albert-Seifried, R. L. Z. Hoye, A. Sadhanala, D. Muñoz-Rojas, J. L. Macmanus-Driscoll, and R. H. Friend, *Adv. Funct. Mater.*, 2014, Accepted.
40. R. L. Z. Hoye, B. Ehrler, M. L. Böhm, D. Muñoz-Rojas, R. M. Altamimi, A. Y. Alyamani, Y. Vaynzof, A. Sadhanala, G. Ercolano, N. C. Greenham, R. H. Friend, J. L. MacManus-Driscoll, and K. P. Musselman, *Adv. Energy Mater. Doi 10.1002/aenm.201301544*, 2014.
41. L. Dunlop, A. Kursumovic, and J. L. MacManus-Driscoll, *Appl. Phys. Lett.*, 2008, **93**, 172111.
42. S. Suh, S. Park, H. Lim, Y.-J. Choi, C. Seong Hwang, H. Joon Kim, and S.-J. Won, *J. Vac. Sci. Technol. A Vacuum, Surfaces, Film.*, 2012, **30**, 051504.
43. A. Holmqvist, T. Törndahl, and S. Stenström, *Chem. Eng. Sci.*, 2013, **96**, 71–86.
44. C. D. Travis and R. A. Adomaitis, *Chem. Vap. Depos.*, 2013, **19**, 4–14.
45. P. Poodt, J. van Lieshout, A. Illiberi, R. Knaapen, F. Roozeboom, and A. van Asten, *J. Vac. Sci. Technol. A Vacuum, Surfaces, Film.*, 2013, **31**, 01A108.
46. P. Poodt, A. Illiberi, and F. Roozeboom, *Thin Solid Films*, 2013, **532**, 22–25.
47. M. B. M. Mousa, C. J. Oldham, J. S. Jur, and G. N. Parsons, *J. Vac. Sci. Technol. A Vacuum, Surfaces, Film.*, 2012, **30**, 01A155.
48. P. Ryan Fitzpatrick, Z. M. Gibbs, and S. M. George, *J. Vac. Sci. Technol. A Vacuum, Surfaces, Film.*, 2012, **30**, 01A136.
49. A. Illiberi, F. Roozeboom, and P. Poodt, *ACS Appl. Mater. Interfaces*, 2012, **4**, 268–72.
50. A. Illiberi, R. Scherpenborg, Y. Wu, F. Roozeboom, and P. Poodt, *ACS Appl. Mater. Interfaces*, 2013, **5**, 13124–8.
51. X. Ren, T. Gershon, D. Iza, D. Muñoz-Rojas, K. Musselman, and J. L. MacManus-Driscoll, *Nanotechnology*, 2009, **20**, 365604.

52. K. P. Musselman, G. J. Mulholland, A. P. Robinson, L. Schmidt-Mende, and J. L. MacManus-Driscoll, *Adv. Mater.*, 2008, **20**, 4470–4475.



Fast air printing of functional oxide films: spatial atomic layer deposition, a new technique with a high potential in the field of low cost photovoltaics.
148x71mm (150 x 150 DPI)

Fast air printing of functional oxide films: spatial atomic layer deposition, a new technique with a high potential in the field of low cost photovoltaics.